Opto-Electronic Advances

Supplementary information

2020, Vol. 3, No. 7

DOI: 10.29026/oea.2020.190040

On-chip readout plasmonic mid-IR gas sensor

Qin Chen[1,*], Li Liang[1], Qilin Zheng[1], Yaxin Zhang[2] and Long Wen[1*]

[1]Institute of Nanophotonics, Jinan University, Guangzhou, 511443, China; [2]University of Electronic Science and Technology of China, Chengdu, 610054, China.

*Correspondence: Q Chen, E-mail: chenqin2018@jnu.edu.cn; L Wen, E-mail: longwen@jnu.edu.cn

This file includes:

Supplementary information for this paper is available at https://doi.org/10.29026/oea.2020.190040

Section 1. Electrical resistance for VO_2 film

In our simulation, the electrical resistance of the VO_2 film versus temperature is from the literature as shown in Fig. S1[1].

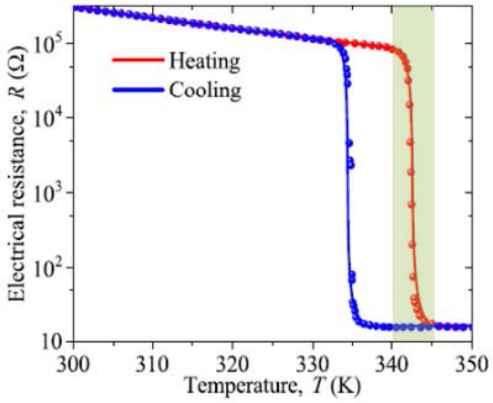

Fig. S1 | The electrical resistance R of VO2 as a function of its temperature.

Section 2. Refractive index of MOF with adsorption of CO_2

MOF is a new type of nanoporous crystalline material consisting of metal ions and organic ligands. It can selectively adsorb certain gas molecules and concentrate them into the nanopores. In Ref.[2], at least 200 times increase of the absorption of CO_2 was observed at various concentration due to the physical adsorption of a type of MOF (zeolitic imidazolate framework, ZIF-8) layer with a thickness of 2.7 μm. Considering the void fraction of ZIFs is approximately 0.47[3], the refractive index of MOF in a protecting gas (Ar) environment can be calculated following the effective material theory

$$n_{\mathrm{MOF}} = 0.53\times n_1 + 0.47\times n_{\mathrm{Ar}}\,, \tag{1}$$

where n_1 is the refractive index of solid ZIF-8 material, and n_{Ar} is the refractive index of Ar at a standard atmospheric pressure. The n_{MOF} is set to be 1.326 in Ref.[2] and the same value is used in our simulation.

As we know, the change of refractive index of gas is directly proportional to the change of the number of gas molecule per unit volume[4],

$$n_{\mathrm{gas}}\text{-}n_0 = kN\,, \tag{2}$$

where n_{gas} is the refractive index of gas, n_0 is the refractive index of vacuum, N is the number of gas molecule per unit volume, and k is a constant. Therefore, the ZIF-8 can concentrate CO_2 molecules by at least 200 times. When this MOF layer is placed in a gas mixture with 10% CO_2 and 90% Ar as the simulation in Fig. 5, its refractive index (real part) can be calculated by combining (1) and (2),

$$n_{\mathrm{MOF}} = 0.53\times n_1 + 0.47\times[1+(n_{\mathrm{CO2}}\text{-}1)\times 10\%\times 200] + 0.47\times[1+(n_{\mathrm{Ar}}\text{-}1)\times 90\%]\,. \tag{3}$$

The imaginary part raised by the CO_2 molecules can be easily calculated by $0.47\times k_{\mathrm{CO2}}\times 10\%\times 200$, where k_{CO2} is the imaginary part of the refractive index of CO_2 obtained from HITRAN web. Please note it is a coarse evaluation of the refractive index of MOF as the pressure, temperature, volume and so on can all change the refractive index. The formula (3) is to give a hint of the influence of MOF on the CO_2 sensing.

Section 3. Gas sensors optimized for the absorption bands of different gases

As discussed in Fig. 2, the resonant absorption of the gas sensor is based on the SPP, whose resonant wavelength is determined by the grating period. Thus, it is easily tuned to match the fingerprint absorption wavelength of various gases to further improve the sensitivity. As shown in Fig. S2, narrowband (Q>250) resonance with high absorption (>90%) can be obtained for various gases such as CH_4, CO_2, CO, SO_2, SF_6 and NO_2 by tuning the structure dimensions. For an extreme optimization, nearly unity absorption with a Q over 1200 is demonstrated for SF_6. In this case, a small amount variation of the gas concentration induces a large change on absorption.

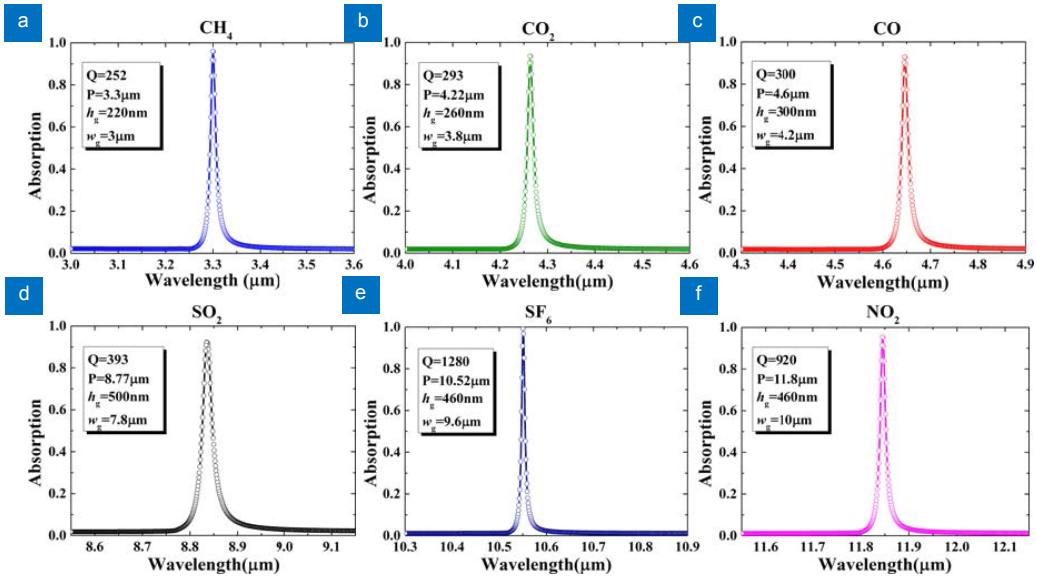

Fig. S2 | Absorption spectra with absorption peaks at the absorption bands for (a) CH_4 at 3.3 μm, **(b)** CO_2 at 4.26 μm, **(c)** CO at 4.65 μm, **(d)** SO_2 at 8.83 μm, **(e)** SF_6 at 10.55 μm, **(f)** NO_2 at 11.85 μm. The structural parameters and the Q factors are shown in the figures.

Section 4. On-chip spectroscopy based on the plasmonic sensor array

In simulation, the spectrum of the broadband source refers to the IR light source in a FTIR spectrometer (MIR8035TM), which is shown in Fig. S3(a). The absorption coefficient of CO_2 is from the HITRAN database[5] as shown in Fig. S3(b). 80 narrowband plasmonic sensors like the one in Fig. 4 are chosen and the spectra are shown in Fig. S3(c), where the pink shadow area indicates the wavelength region in the spectrum reconstruction in Fig. 6.

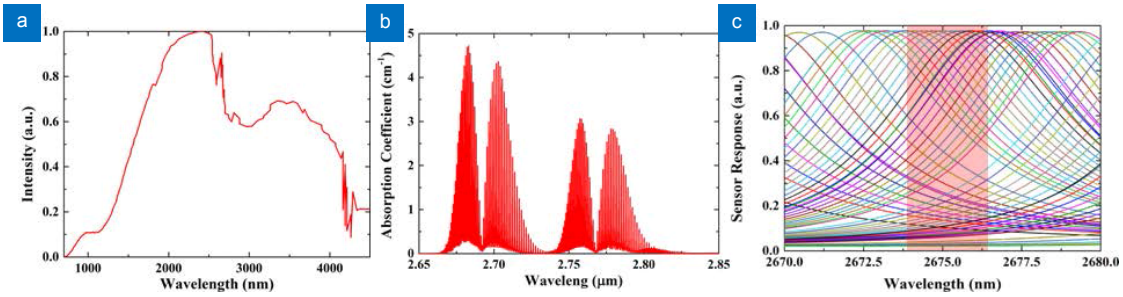

Fig. S3 | (a) The spectrum of the broadband source used for gas molecular absorption spectrum reconstruction. **(b)** The absorption line intensity of CO_2 is from the HITRAN database. **(c)** Spectra of 80 narrowband plasmonic sensors.

Section 5. Size effect of plasmonic structure in mid-IR gas sensor

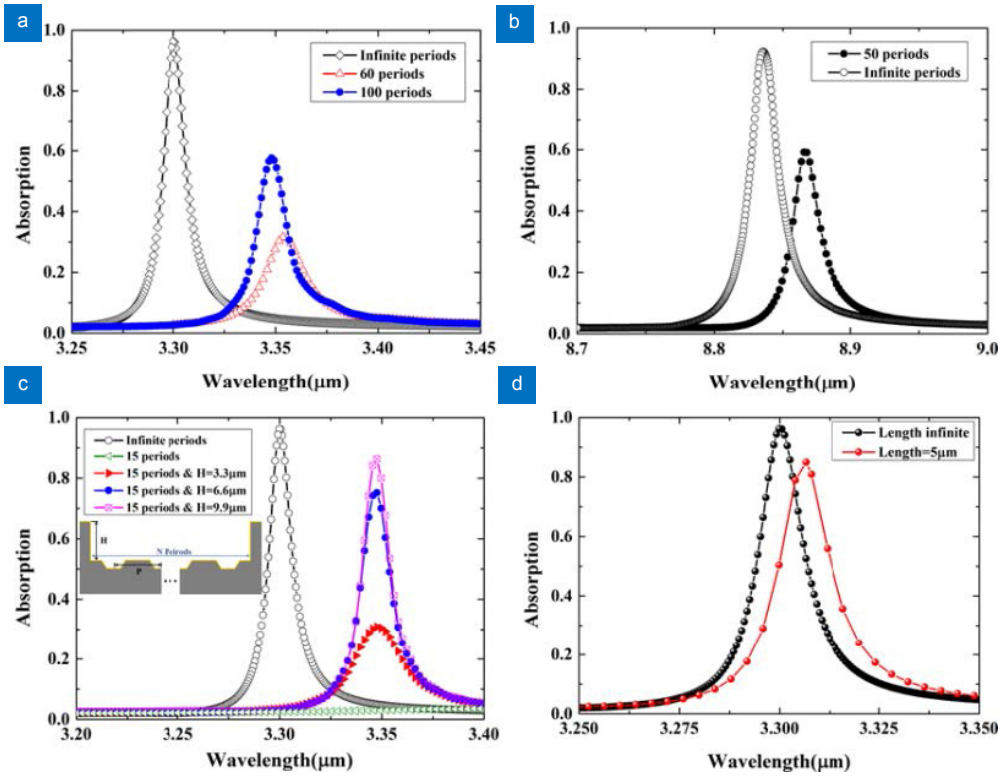

Fig. S4 | The absorption spectra of the plasmonic structures shown in Fig. 2 with different number of grating periods at the resonance around (a) 3.3 μm and **(b)** 8.8 μm. **(c)** The absorption spectra for the structures (with 15 gratings) with reflectors at both ends for different reflector heights. **(d)** Effect of the grating length along the z direction (Fig. 1) on the absorption spectrum. Spectra of the periodic structures are shown for comparison.

Reference

1 Ordonez-Miranda J, Ezzahri Y, Joulain K, Drevillon J, Alvarado-Gil J J. Modeling of the electrical conductivity, thermal conductivity, and specific heat capacity of VO_2. *Phys Rev B* **98** (7), 075144 (2018).

2 Chong X Y, Zhang Y J, Li E, Kim K J, Ohodnicki P R, Chang C H, Wang A X. Surface-Enhanced Infrared Absorption: Pushing the Frontier for On-Chip Gas Sensing. *ACS Sensors* **3** (1), 230 (2018).

3 Thornton A W, Simon C M, Kim J H, Kwon O, Deeg K S, Konstas K, Pas S J, Hill M R, Winkler D A, Haranczyk M, Smit B. Materials Genome in Action: Identifying the Performance Limits of Physical Hydrogen Storage. *Chem Mater* **29** (7), 2844 (2017).

4 Omini M. Optical properties of liquids under pressure. *J PHYS I* **39** (8), 847-861(1978).

5 Rothman L S, Gordon L E, Barbe A, Chris Benner D, Bernath P F, Birk M, Boudon V, Brown L R, Campargue A, Champion J-P, et al. The HITRAN 2008 molecular spectroscopic database. *J Quant Spectrosc RA* **110** (9-10), 533 (2009).